# Understanding a Bisferrocene Molecular QCA wire

Azzurra Pulimeno, Mariagrazia Graziano, Aleandro Antidormi, Ruiyu Wang, Ali Zahir, and Gianluca Piccinini

Dipartimento di Elettronica e delle Telecomunicazioni, Politecnico di Torino, Italy

**Abstract.** Molecular QCA are considered among the most promising beyond CMOS devices. Frequency as well as self-assembly characteristics are the features that make them most attractive. Several challenges restrain them for being exploited from a practical point of view in the near future, not only for the difficulties at the technological level, but for the inappropriateness of the tools used when studying and predicting their behavior.
In this chapter we describe our methodology to simulate and model sequences of bisferrocene molecules aimed at understanding the behavior of a realistic MQCA wire. The simulations consider as variables distances between successive molecules as well as different electric field applied (in terms of input and of clock). The method can be used to simulate and model also other more complex structures, and perspectives are given on the exploitation of the achieved results.

## 1 Introduction on molecules for QCA

### 1.1 Molecular implementation

Molecules, with their moving charges, present well-suited properties to perform information storage and processing in the ways expressed by the QCA paradigm [1]. Molecular charges can localize, under the influence of an external field, in determined locations of the molecule, resulting in different spatial charge configurations. Thus, molecular systems can be exploited as basic cells for binary computing: each configuration encodes a binary state and a switch from a state of the cell to another results from a charge flow through tunnelling paths within the molecule itself. Molecular sites where charge localization occurs are called redox centers and represent the dots of the QCA device; they are effectively capable of attracting or releasing an electron thus becoming positively or negatively charged.

Since a molecule is neutral, a better performance is obtained with the oxidized and reduced forms of the same molecule; in the oxidized molecule, an electron is missing and its net charge is positive; in the reduced form, the molecule has gained an electron picking up a negative net charge.

A simplified scheme of an oxidized molecule is shown in Figure 1: an electron is free to move along the tunneling path and localize into one of the two redox

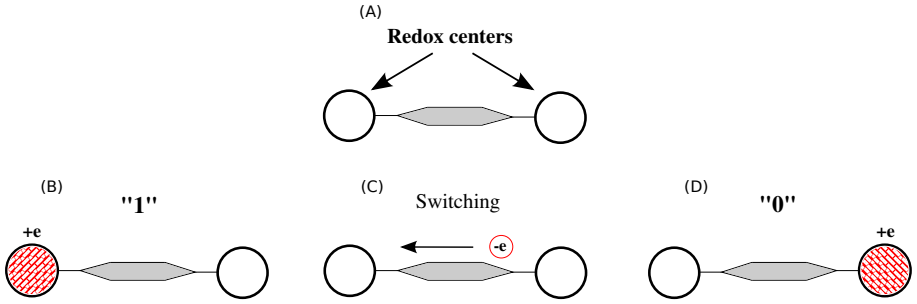


**Fig. 1.** Molecular implementation: (A) molecule sketch; (B), (C) and (D) logic encoding and switching in case of oxidized molecule.

sites available (the circles in this simplified representation). Encoding of binary information is related to the charge configuration of the cell: for example, when the positive charge is in the redox site on the left (the circle with internal pattern in this simplified representation, Fig. 1(B)), the cell is, for example, in a logic 1 state. When the positive charge is located on the right site (patterned circle on the right, Fig. 1(D)), then the molecule is in the 0 state. These charge configurations are represented in Figure 1, along with the switching state corresponding to the free charge moving along the tunnelling path from one dot to the other (Fig. 1(C)). The intermediate symbol (stretched exagon) represents a part of the molecule slightly active from the electrostatic point of view, but acting like a channel to favor charge movement and as separator to favour charge localization in one of the two dots.

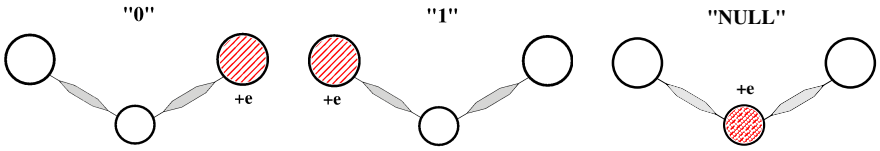


**Fig. 2.** State encoding of a 3-dot molecule.

The encoding scheme chosen in the previous example is ostensibly arbitrary, since other choices are possible. No choice can be made, instead, on the number of different possible configurations of charge within a given molecule, and correspondingly on the number of encoded states. The motivation for having more charge configurations in a single molecule resides in the mode of switching adopted in circuits with many QCA cells. A mode of switching consists in a procedure with several steps which allow the QCA cells to switch their state thus transmitting or processing the information. To avoid metastability prob-

lems, the so-called adiabatic mode of switching has been divised and a single cell must dispose of six dots [2, 3]. Consequently a molecule must have three redox centers, as sketched in Figure 2. The third redox center is used to encode the logic NULL state which corresponds to the charge occupying the central dot. A molecule with three active dots reproduces a half-QCA cell and can be completed to form a whole cell aligning another molecule on its side (Figure 3). The two half-cells interact through the electrostatic forces among the free charges which tend to localize within each molecule in order to minimize the relative potential energy. This configuration clearly recalls the theoretical QCA structures based on squared cells able to capture charges in the dots along the diagonal of the square [1].

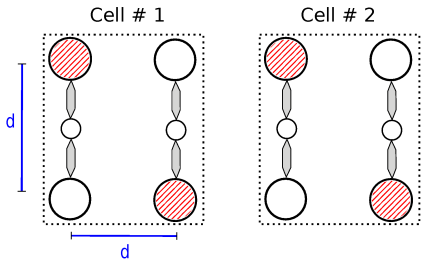


**Fig. 3.** Complete QCA cell and interaction between cells (top view).

### 1.2 Candidates molecules

On the applicative point of view, the greatest effort in developing molecular QCA cells is in the quest for molecules with proper features as computing elements. The ideal molecule, indeed, encompasses many properties which reveal to be strictly necessary.

Many molecules present geometrical structures which limit the molecule itself to be used only in the gas phase or in solution; this is mainly due to the lack of a binding element for deposition on substrates. Consequently, practical QCA molecules should poses the functional groups that allow attachment and orientation on a surface.

As already mentioned before, a suitable molecule should have at least three redox centers in order to encode the NULL states, introduced for energy and stability reasons.

Finally, a simple and reliable mechanism is necessary to set and read molecular states at the edge of a molecular array. Devising solutions to this problem is a major issue, given the actual absence of instruments capable of revealing the motion of single charges on nanometer scale.

Many molecules have been presented and analyzed. Most of them are ideal [4–6, 9–12, 19] and their functionalities have been tested via computer simulation but never synthesized. Others, instead, are real molecules synthesized ad hoc for QCA purposes [7, 8, 13, 14, 20, 21] and for some of them even early preliminary experiments have been carried out.

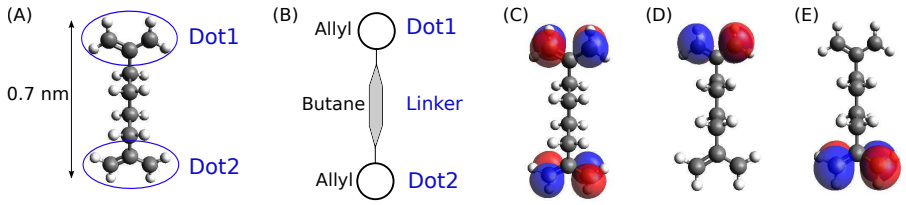


**Fig. 4.** The diallyl butane molecule: (A) structure, (B) scheme and (C, D, E) orbital localization.

The first molecule which has been proposed for QCA computing is the diallyl butane [6]. As shown in Figure 4, it consists of two allyl groups connected by a butane bridge. The most suitable form for the molecule is the cationic one, where a positive charge is free to move inside the molecule. The corresponding unpaired electron can occupy one of the opposite allyl end-groups, which represent the dots (circled in Figure 4(A) and sketched in Figure 4(B)); the tunnelling path between these redox centers is consequently given by the butane bridge. When the charge tunnels from one end to the other, a different charge configuration of the molecule is obtained and a different highest occupied molecular orbital (HOMO) is realized (Figures 4(C,D,E)).

A molecular orbital is an eigenfunction of the hamiltonian operator for a molecular system, corresponding to a determined value of energy (eigenvalue) of the molecule. According to quantum mechanics, this function represents the spatial probability of finding an electron in a specific region of space with that energy. Thus, from a molecular orbital the most probable location of an electron can be evaluated. Moreover, each molecular orbital can be occupied by two electrons with opposite spin and, in general, all the electrons tend to arrange themselves in order to fill the orbitals starting from the one with the lowest energy. In this sense, the HOMO is the last energy level occupied by the available electrons and it has the highest energy.

In the diallyl butane cation an electron from the HOMO is removed, consequently the HOMO represents the localization of the unpaired electron. The possible HOMO conformations are shown in Figure 4(C,D,E): in Figure 4(D) the HOMO is simmetrically delocalized between the two allyl groups favoring the electron occupation neither of the top nor of the bottom group: it corresponds to an undefined state. In Figure 4(B) and (E) instead, the HOMO (and thus

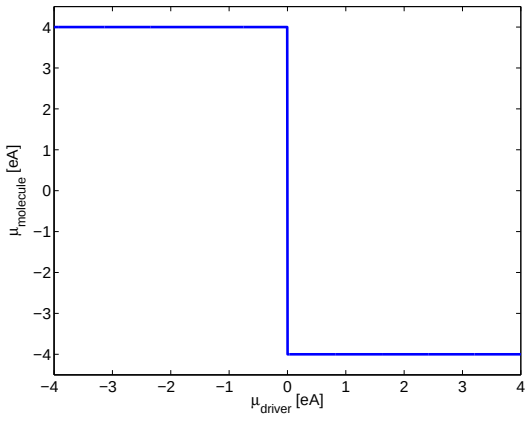


**Fig. 5.** The single-molecule response of the diallyl butane molecule to a point charge driver.

the charge) is localized on one of the two dots, so these configurations could represent the logic states 1 and 0.

All these HOMO configurations differ for the dipole moment generated in the molecule from the charge localization: a positive moment in Figure 4(C), a negative one in Figure 4(E). Such a quantitative parameter, evaluated multiplying the electron positive charge and its distance from the center of the molecule, offers a way to analyze the molecular response when a change in the Coulomb field produced by neighboring molecules occurs. A QCA molecule is indeed expected to respond in non-linear way to the external perturbations, switching from one state to another as demonstrated in [6]. This nonlinear behaviour is shown in Figure 5 where the dipole moment of the molecule is shown as a function of the external dipole moment, considered as input of the system. The dipole of the molecule has opposite sign with respect to the driver dipole moment; thus the molecule interacts properly with the neighboring molecules assuming the opposite state.

The diallyl butane molecule consititues only a half QCA cell; a whole QCA device can be obtained aligning two molecules along the axis thus forming a squared structure. Although very performing as a QCA device for its good charge confinement and non-linear molecular response, the diallyl butane is not suitable for real application. It lacks the possibility of encoding a NULL state for clock issues and has no binding element to be placed on a substrate following a specific layout. Other molecules should be devised which could overcome these limitations.

The decatriene [10] is one possible candidate to overcome the deficiencies of diallyl butane: its molecule presents three dots (a sketch of its structure is reported in Figure 6). Each dot is an ethylene groups (the circle) and equivalently

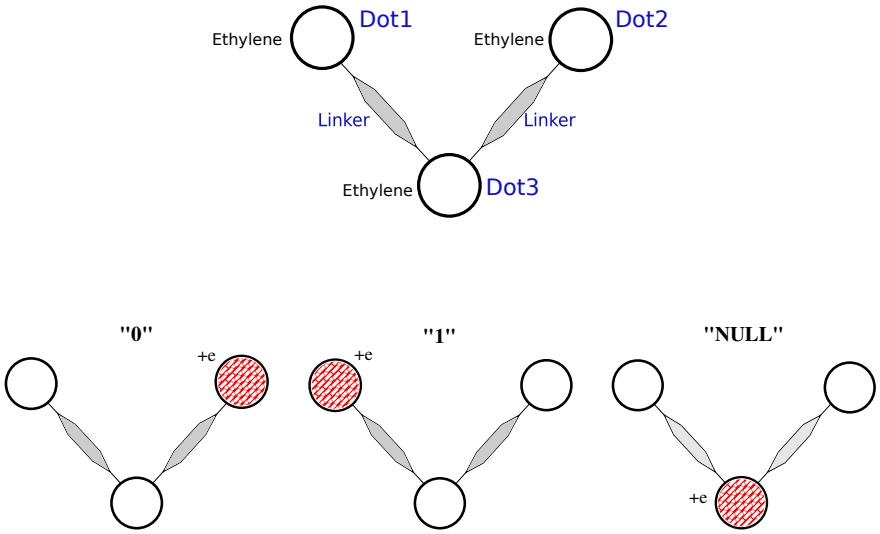


**Fig. 6.** The decatriene: structure (top) and state encoding (bottom).

to the diallyl butane, no element is unforntunately able to allow attachment of the molecules on a surface.

The redox centers of the decatriene confine charge in the molecule according to three configurations (schematically reproduced at the bottom of Figure 6): a simple correspondence can, then, be established among these charge conformations and logic states 0, 1 and NULL. In the ground-state, with no electric field applied, the molecule configuration is the one encoding the NULL state. When an electric field is applied in the vertical direction (called clock field) the molecule ends up in an excited state: a simultaneous application of another electric field parallel to the active dot axis (called switching field) implies the charge localization on one of the two dots, depending on the sign of the switching field, leading the molecule into the logic state 0 or 1.

One of the real molecules proposed as QCA device is a mixed-valence complex based on one iron atom (Fe) and one ruthenium atom (Ru) [7]. The molecule schematic structure is shown in Figure 7(A): the two dots are vertically organized and are given by the metal atoms, while the ending nitrogen atom (N) plays the role of binding element allowing the molecule to be attached to a silicon substrate. Its functionality properties have been verified placing the oxidized form of the molecule between a silicon surface and a mercury tip, thus realizing a plate capacitor. Applying different voltages (electric fields) the free charge in the molecules moves from one dot to the other generating a change in the differential capacitance. By measuring a change in the differential capacitance an experimental demonstration of the charge motion inside the molecule has been given as a consequence of the external field (Figure 7(B)).

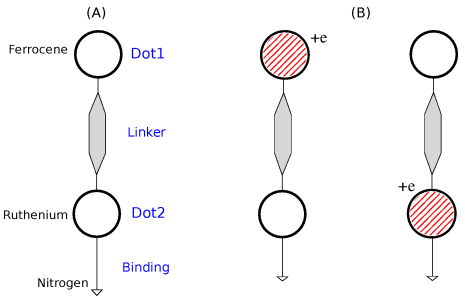


**Fig. 7.** The Fe-Ru mixed valence complex: (A) structure and (B) state encoding.

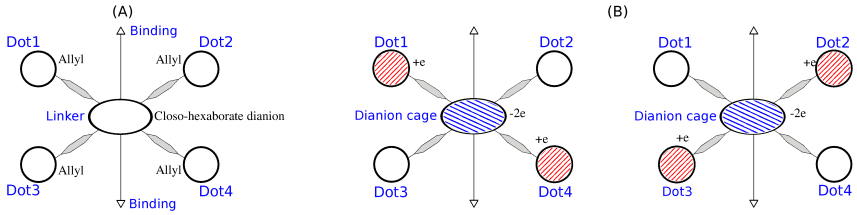


**Fig. 8.** The mixed-valence zwitterion: (A) structure and (B) state encoding.

Another real molecule proposed in literature is a mixed-valence complex based on iron atoms (Fe) [21]. This molecule is called meta-Fe2: the active dots are represented by two metal-ligand units, each composed of a cyclopentane (Cp) and in iron atom (Fe), while an ethynil linker connects them to a central benzene ring. Scanning Tunnelling Microscope (STM) imaging has revealed that the presence of perturbations in the molecular environment leads to a charge confinement inside the molecule in cationic form.

All the molecules already discussed need to be oxidized or reduced in order to employ their nonzero net charge to realize different charge configurations encoding binary information. As a consequence, particular attention has to be payed to control redox processes. The zwitterion, a molecule which incorporates a donor or acceptor site, permits to overlook such difficulties. This special site releases or attracts an electron, generating a free mobile charge in the molecule while preserving the overall neutrality.

A practical example of mixed-valence zwitterion based on boron clusters has been proposed as QCA device [11]. The octahedral cage of a closo-hexaborate dianion (sketched in Figure 8(A)) is used as central linker group for four redox centers, while other two axial linker could be used to bind the molecule on a substrate. The boron cage attracts two electrons from two antipodal active dots, thus becoming doubly negatively charged; two choices of opposite dots are possible, subsequently two binary states can be encoded, as shown in Figure 8(B).

Differently from the previous molecules, this molecule implements a complete QCA cell.

### 1.3 The bisferrocene molecule

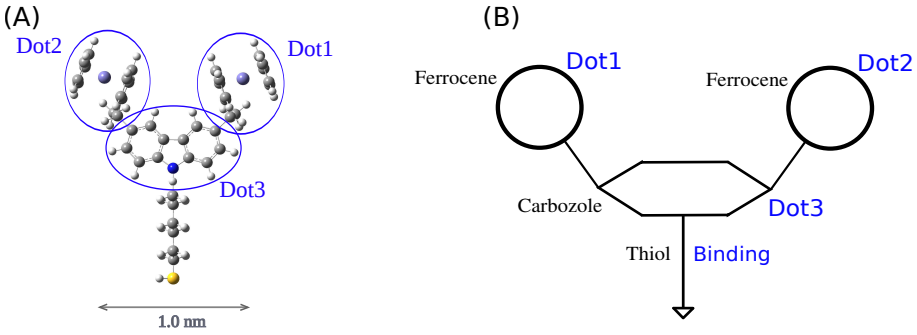


**Fig. 9.** The bis-ferrocene molecule: (A) structure and (B) scheme.

In the continuous research for molecules suitable to be employed in QCA computing, recently a new candidate molecule hase been proposed and studied: the bis-ferrocene molecule ([13–18]). This molecule, shown in Figure 9 is constituted by two ferrocenes, functioning as redox centers, and a carbazole bridge which acts as third dot for the NULL state. An alkyl chain is also present, which guarantees the attachment to a gold surface. The bis-ferrocene molecule is capable of realizing a QCA half-cell, thus two molecules aligned are necessary for an entire cell.

Its features have been demonstrated through teoretical and experimental analysis [13, 14]. Three isomers of the molecule have been synthesized: two diastereoisomers (the (S,S) and (R,R), chiral compounds) and the mesoisomer. Oxidation has also been performed chemically, with the introduction of iodine atoms (I) as counterions in the solution, and electrically, through cyclic-voltammetry (CV).

The possibility of binding bisferrocene molecules on a gold surface has also been demonstrated, as proved by the results of STM imaging shown in [14]. STM characterization has revealed the presence of structures with one and two lobes with almost the same density; further analysis has allowed to associate them with the (R,R and S,S) stereoisomers and (R,S) meso isomer, respectively.

The capacity of the bis-ferrocene molecule to correctly respond to a change in local electric field has been verified on the (R,S) *syn* isomer in its oxidized form [14]. In particular, after computing the electron density for an isolated molecule (the driver) in its cationic state, the electron density of a second molecule (the driven molecule) was deduced in presence of the point-charge electrostatic field

of the first molecule. As expected, the external field seems to move the internal positive charge on the ferrocenes generating different charge configurations [14].

## 2 Methodology for the analysis of molecule and ensamble of molecules

This section describes a possible methodology to evaluate and simulate all the important parameters necessary for molecular QCA devices. It is aimed to represent both the bis-ferrocene features as QCA devices and the feasibility of computing with molecular QCA. Additionally, also the methodology for analyzing defects concerning QCA wire fabrication is provided.

The study is organized in two stages, as in the scheme in figure 10: **Stage I**, where ab-initio simulations are performed under different conditions as detailed in section 2.1; and **Stage II**, where electrostatic equations and models are set up in order to define new figures of merit to describe the QCA molecular system (see section 2.2) and to understand its potentials from an electronic point of view.

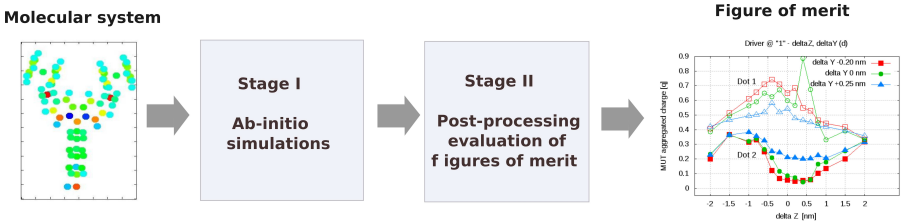


**Fig. 10.** A two stages analysis from molecular systems to device-level figures of merit.

### 2.1 Stage I) Ab-initio simulations

The computations and evaluations of the electronic structure and properties based on ab-initio simulations we performed (see Fig. 11) focus mainly on the laws of quantum mechanics and a set of physical constants (the speed of light, masses and charges of electrons and nuclei, Plank's constant).

They are based on the theory from the first principle and are highly accurate and, as a consequence, computationally intensive. In order to characterize a molecule as QCA device, a set of ab-initio simulations could be performed on different conditions of molecular systems, by defining proper methods and basis sets.

**S-I A) Single oxidized and neutral molecule simulation** The binary information of the molecular QCA system could be evaluated by using the figure of

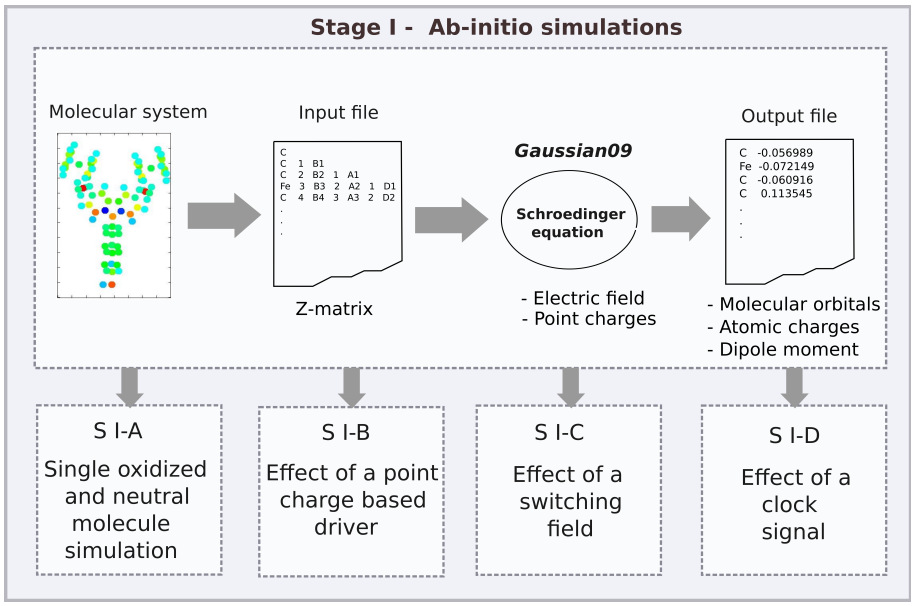


**Fig. 11.** Stage I) Ab-initio simulations: from molecular system chemical inputs to molecular system energetic and electrostatic quantities.

merit of highest occupied molecular orbital (HOMO), as mentioned in [6, 9, 10]. While based on this, in order to take clearly the electronic point of view about the molecular QCA, some new figures of merit could be used to analyze the QCA molecule, both in its neutral and oxidized or reduced form. In particular, the charge distribution of the molecule has to be evaluated when the molecule is subject to a write-in system (like an electric field as described in [16]).

**S-I B) Effect of a point charge based driver** Regrading the interaction between molecules, the methodology discussed here involves the simulation of a system considered as a complete QCA cell: it contains an ideal driver represented by point charges located at the distance $d$ from the molecule as shown in Figure 12(A). In this way, the ideal driver could emulate the other molecule of the complete QCA cell. In the case of neutral molecule, the point charges of the driver molecule are two and opposite (which are $+1e$ and $-1e$), placed respectively at the position of the two working dots, imitating an internal charge splitting that preserves the neutrality of the driver molecule. Thus, putting the polarized ideal driver next to the molecule and changing the state of the driver (swapping the position of the two point charges), it is possible to check whether or not the target molecule changes its logic state as well.

On the the other hand, in the case of oxidized molecule, only one positive charge ($+1e$) is considered to simulate the ideal driver. In particular, the point charge is located on one of the two dots of the driver, according to its logic

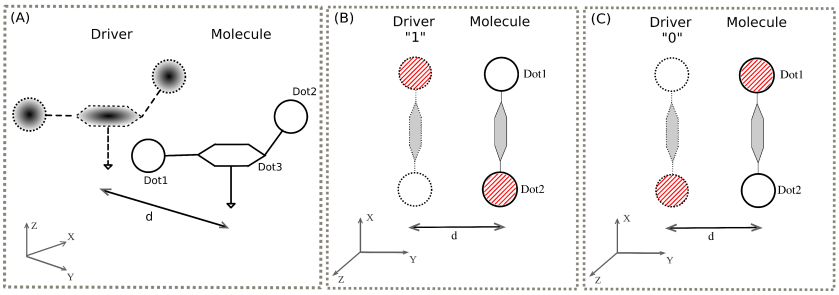


**Fig. 12.** Model of driver-molecule interaction.

state. In this way, considering the case of driver at logic 1 (as represented in Figure 12(B)), the charge distribution on the target molecule could be evaluated by means of ab-initio simulations. Then, switching the driver to a logic 0 (as represented in Figure 12(C)) the target molecule is expected to switch, as well, in the opposite state.

The amount of charge mentioned here is always referred to the elementary charge ($e$) as unit of measurement and hereinafter the $e$ will be neglected for sake of brevity.

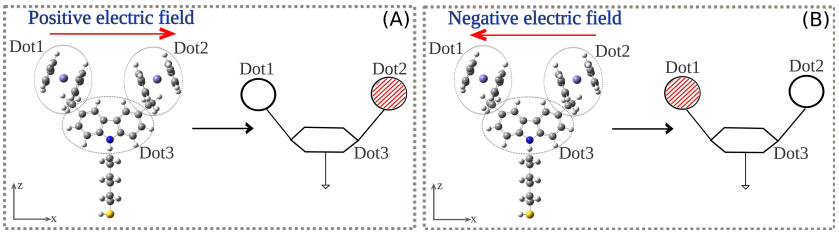


**Fig. 13.** Model of write-in system.

**S-I c) Effect of switching field** As already demonstrated in [16], the electric field generated by the write-in system of the molecular QCA cells is called *switching field* and the direction of the switching field is considered to be parallel to the working dot axis.The electric field should force the charge to localize in one of the two active dots and thus writing of a logic state in a QCA molecule. By changing the sign of the switching field, the charge localization could be led in the opposite dot and , as a consequence, the molecule should change its logic state. The write-in system could be modeled and simulated applying a uniform electric field to the molecule as shown in Figure 13 and the effective-

ness of this method could be evaluated computing the charge distribution of the molecule: considering for example the oxidized bis-ferrocene and applying a positive switching field (Figure 13(A)) the free positive charge should localize on Dot2; while in case of negative switching field (Figure 13(B)) the charge should be on Dot1.

**S-I D) Effect of clock signal** As mentioned before, in order to realize the adiabatic switching, the clock signal should be taken into account in the simulation. It is important to analyze the possibility of enhancing or hindering the communication between nearby molecules. In case of three-dot molecules, the clock signal could be implemented by applying an electric field along the vertical axis of the molecule (like the Z axis as illustrated in Figure 14(A) for the bis-ferrocene molecule). The analysis could be performed also in presence of a polarized driver for both neutral and oxidized form of the target molecule. This means simulating the molecule subject to the simultaneous effects of a clock signal and a polarized driver, in order to evaluate its capability to interact with a nearby molecule.

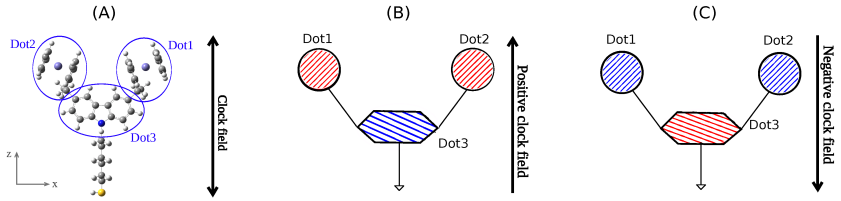


**Fig. 14.** Application of a clock signal to the bis-ferrocene molecule.

## 2.2 Stage II) Post-processing

Picture 15 gives an overview of the second stage of our analysis. Starting form the ab-initio simulation results obtained in the various conditions, we elaborate methods to reckon more usable quantities defined in the following.

**S-II A) Charge analysis** In order to model the molecular QCA system from an electronic point of view, it is still necessary to evaluate the results of the ab-initio simulations by defining new figures of merit. Thus, instead of focusing only on the HOMO of the molecule (as mainly done in the chemical approach proposed in literature), a new figure of merit, the *atomic charge* of the molecule, could be considered in different operating conditions (ground state and biasing). The atomic charge could be computed by means of ab-initio simulations using the Merz-Singh-Kollman (MK) approximation scheme (also called ESP) [23].

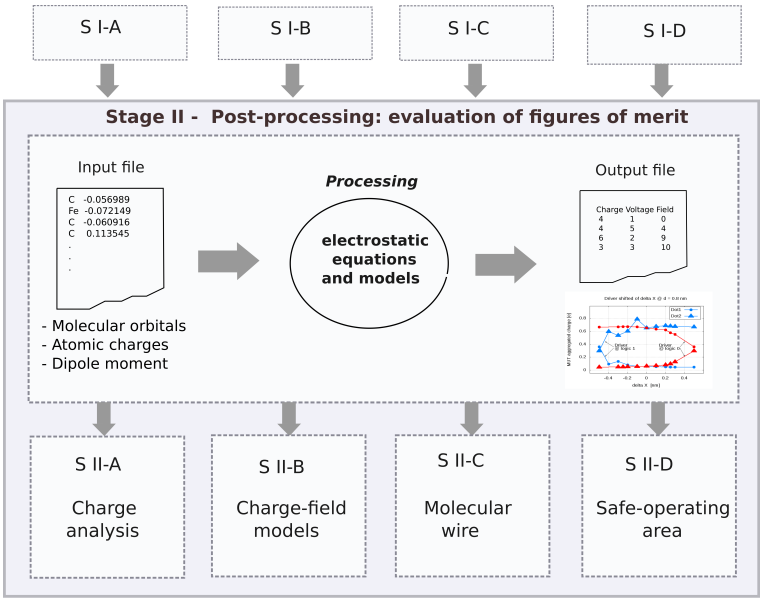


**Fig. 15.** Stage II) post-processing: from ab-initio to device level figures of merit.

Furthermore, another new quantity defined as *aggregated charge* could be computed, based on the given atomic charges of the molecule. Particularly, the charge of the entire working dots (the two ferrocenes and the carbazole) and of the thiol group are computed simply summing the atomic charge of all the atoms that form each redox center. Figure 16 illustrates the methodology chosen to calculate the aggregated charges: the left picture shows the bis-ferrocene atoms (filled circles) colored in different ways according to the atomic charge of each atoms; summing all the atoms included in each part of the molecule (the dots circled in the figure and the thiol), it is possible to model the molecule with a system of point charges. In Figure 16, only the three dots are considered to model the charge distribution of the molecule and so the bis-ferrocene is modeled with three charges (Q1, Q2 and Q3) that correspond to the three dots (Dot1, Dot2 and Dot3, respectively). This is because of the fact that the atomic charge itself is a theoretical approximation used to easily demonstrate the charge distributed on the molecule instead of an exact physical quantity. Although since the definition of *aggregated charge* is generated by means of summing the atomic charge in a particular way, it could demonstrate the charge distribution inside a molecule from a macroscopic point of view and at the same time, from the point of view of an application, it could also be a readable quantity (as discussed in [16]). Hereinafter, when dot charge is referred, it means the reference to the aggregated charges of the corresponding dots.

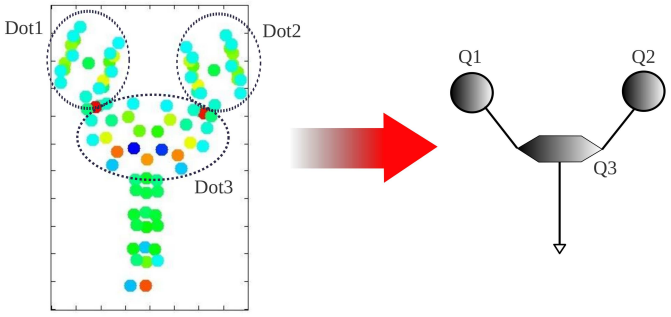


**Fig. 16.** Definition of the aggregated charge for each dot.

**S-II B) Charge-field models** As long as the the aggregated charges of the molecule under different bias conditions (point charge based driver, switching field or clock signal) is obtained by means of simulations, it is possible to compute the electric field generated by the charge distribution of the molecule at any specific working point through mathematical equations developed in MatLab/Octave. Particularly, a single charge $+q_1$ is considered to be placed at $(x_0, y_0, z_0)$, and the electric field $E(x, y, z)$ can be evaluated by means of a positive test charge $+q_t$ positioned in $(x, y, z)$. The distance $\overrightarrow{r_1}$ between $q_1$ and $q_t$ and its modulus $r_1$ are defined as

$$r_1 = \sqrt[2]{(x - x_0)^2 + (y - y_0)^2 + (z - z_0)^2} \tag{1}$$

$$\overrightarrow{r_1} = r_1 \cdot \widehat{r} \tag{2}$$

where $\widehat{r}$ is the unit vector of the axis that includes the space point of $q_1$ and $q_t$. Following the Gauss law, the Coulomb force $\overrightarrow{F_1}$ experimented by the test charge can be evaluated as

$$\overrightarrow{F_1} = \frac{1}{4\pi\epsilon_0} \frac{q_1 \cdot q_t}{r_1^2} \cdot \widehat{r}. \tag{3}$$

Then, the electric field generated by $q_1$ and measured by the test charge is computed as

$$\overrightarrow{E_1} = \frac{\overrightarrow{F_1}}{q_t} = \frac{1}{4\pi\epsilon_0} \frac{q_1}{r_1^2} \cdot \widehat{r}. \tag{4}$$

Considering a system of N point charges, the different forces related to the multiple charge distribution of the whole system affect the test charge. This effect could be summarized by defining a total force calculated by

$$\overrightarrow{F_{tot}} = \sum_{i=1}^{N} \frac{1}{4\pi\epsilon_0} \frac{q_i \cdot q_t}{r_i^2} \cdot \widehat{r} \tag{5}$$

and so the equation for the total electric field becomes

$$E_{tot}(x,y,z) = \frac{\overrightarrow{F_{tot}}}{q_t} = \sum_{i=1}^{N} \frac{1}{4\pi\epsilon_0} \frac{q_i}{r_i^2} \cdot \widehat{r}. \tag{6}$$

Finally, considering a generic test charge placed at a generic point of the space $(x, y, z)$, the three component ($E_x$, $E_y$ and $E_z$) of the electric field generated by a system of point charges are given by

$$E_x(x,y,z) = \sum_{i=1}^{N} E_{xi}(x,y,z) \tag{7}$$

$$E_y(x,y,z) = \sum_{i=1}^{N} E_{yi}(x,y,z) \tag{8}$$

$$E_z(x,y,z) = \sum_{i=1}^{N} E_{zi}(x,y,z). \tag{9}$$

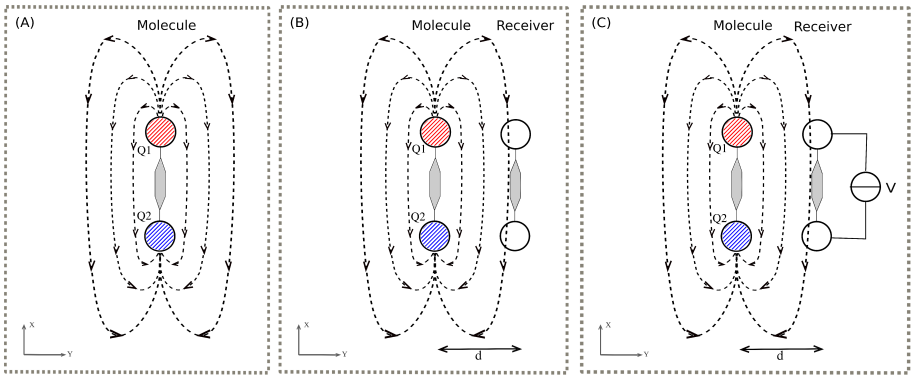


**Fig. 17.** Definition of the generated electric field and the equivalent voltage at the receiver.

Following this procedure, once the aggregated charges of the molecule in a specific condition is obtained, it is feasible to compute the electric field generated by this system of charges (Figure 17(A)) at any points in the space that surrounds the molecular. Just as depicted in Figure 17(B), the electric field is "measured" putting an ideal receiver nearby the molecule with the ideal distance from it to form a squared cell. In order to get the measurement of the electric field, it is necessary to define a new quantity that is called *equivalent voltage at the receiver* (see Figure 17(C)). In particular, the equivalent voltage at the receiver could be computed by considering the component of the electric field parallel to the molecule and integrating it along the width of the molecule.

**S-II C) How to simulate a molecular wire** After characterizing the single bis-ferrocene molecule as QCA devices, it is important to simulate a molecular QCA wire made of oxidized bis-ferrocene molecules. For realizing it, an iterative method could be adopted as sketched in Figure 18. In particular, the write-in system is applied simulating the input molecule (Molecule 1 in Figure 18(A)) under the effect of an electric field (also named switching field). Thus, the logic state of the first molecule is given by the charge distribution and the dot charges are computed. Then, they could be used as the driver for the second molecule (Molecule 2) of the wire. So, the second bis-ferrocene molecule is simulated in presence of a driver, whose charge distribution emulates the logic state of the Molecule 1. In this way, the charge distribution of Molecule 2 is computed and used as driver again for the following cell (Molecule 3) and so on. As depicted in Figure 18(B), at a generic point of the wire the charge configuration of *Molecule i* is computed as the response of *Molecule i-1*, while assuming that the *Molecule i* is in the neutral state (charge delocalized) at the beginning and ready to switch its logic state under the effect of *Molecule i-1*. As a result of that, the aggregated charges (D1, D2 and D3) of the (*Molecule i*) become the driver system of its nearby molecule (*Molecule i+1*) in the following step of information propagation. By iterating this method for all the molecules on the wire, it is possible to simulate the information propagation through the wire.

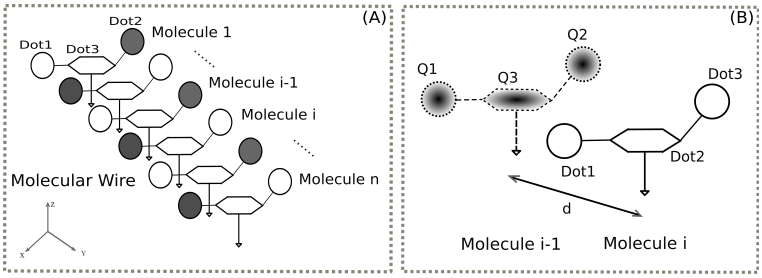


**Fig. 18.** Simulation of a molecular QCA wire made of bis-ferrocene molecules.

**S-II C) How to create SOA for molecules** In order to experimentally demonstrate the QCA functionalities, a bis-ferrocene molecular wire like the one in Figure 18(A) should be fabricated, using on a gold nanowire upon which the molecules can be bonded through the thiol element [16]. During the technological processes, possible fabrication defects may happen [18]. For this reasons, it is important to classify the possible defects and analyze the effects of these defects on the molecular wire, generating thus a Safe Operating Area (SOA) that highlights the fault tolerance of the molecular QCA wire.

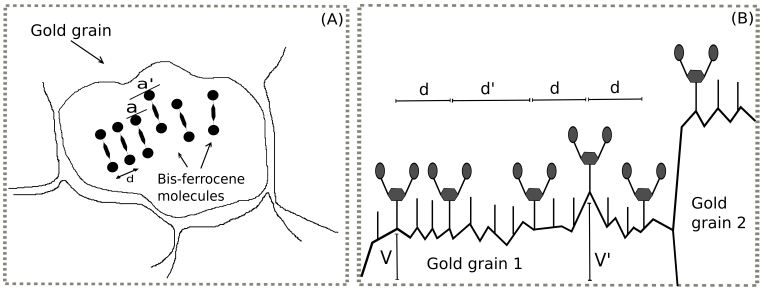


**Fig. 19.** Fabrication defects in the case of a QCA wire made of bis-ferrocene molecules. (a) Top view of a gold grain after molecule deposition: misalignment and tilt defect are sketched. (b) Section of a bis-ferrocene SAM on gold: vertical shifts may occur due to the roughness inside a gold grain or at the interface of two grains; higher molecule-molecule distance is caused by the number of hexane-dithiol elements.

**Defects classification** As mentioned above, some defects may occur when fabricating the gold substrate and after depositing the molecules on the gold nanowire. These defects are schematically classified in Figure 19: misalignment of two nearby molecules, due to the gold grain irregularity or the (Fig. 19(A)); a variation in the vertical distance between the active dot axis of two nearby molecule, as a consequence of the gold layer roughness (Fig. 19(B)); different distances between two nearby molecules, due to the different number of spacer placed in between them (Fig. 19(B)). These defects might cause faults and misbehaviors of the cells in the molecular wire.

**Methodology** In order to perform a fault tolerance analysis in case of a molecular QCA wire, a methodology that could be adopted focuses on a a part of the molecular wire made of the following elements: an ideal driver emulated with the point charge system as described before, a bis-ferrocene molecule ( defined as molecule under test, MUT) and an ideal receiver that acts as third molecule. In particular,the bis-ferrocene is considered in its oxidized form (a positive net charge) and so the ideal driver is modeled with a single positive point charge. When no defects occur (as in the ideal case), the driver is located at an ideal distance $d$ equal to the distance between Dot1 and Dot2 of MUT (equal to 1.0 nm), so that a squared QCA cell is formed along with the receiver and the MUT. Furthermore, the logic state of the driver is given by the position of the positive point charge as shown in Figure 20: when it is localized on Dot1, the driver is in the logic state 1 (Figure 20(A)); while, the charge localization on Dot2 encodes the logic state 0 (Figure 20(D)). SO, the MUT is affected by the presence of a polarized driver and, as consequence, should rearrange encode a logic state opposite to the one of the driver, according to its internal charge distribution (Figure 20(B) and (E)). The dot charges of the MUT ($Q1$ and $Q2$) in a specific logic state generate an electric field as shown in Figure 20(B) and (E), that at the same time affects the receiver with the above mentioned equivalent voltage.

As a consequence, the effect of the equivalent voltage should be such that it lead the receiver in a logic state opposite to the one of MUT, letting thus the information propagate along the wire.

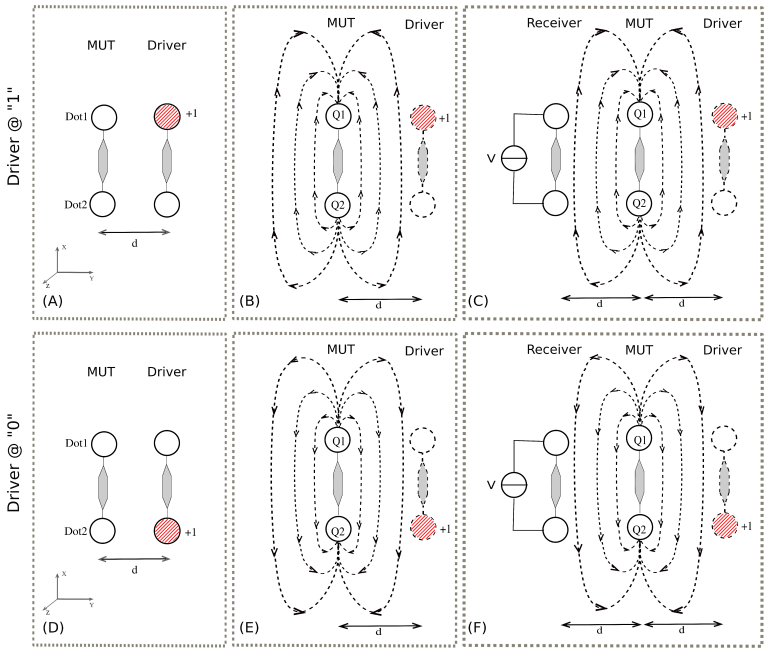


**Fig. 20.** Methodology scheme for the fault tolerance evaluation in case of molecular QCA wire.

Regarding the real fabrication defects that may happen, they could be modeled varying the position of the driver with respect to the MUT as sketched in Figure 21: the misalignment between the driver and the MUT that occurs along the dot axis is defined as $X - displ$, since in the ab-initio simulation the two working dots located along X axis; the variation of the driver-MUT distance with respect to the ideal distance $d$ is called $(Y - displ)$; the vertical displacement of the driver from the ideal position is defined as $(Z - displ)$.

Once the charge distribution of the MUT is obtained for each case of driver displacement, the electric field generated by these charge distributions could be computed and measured at an ideal distance $d$ of 1.0 nm from the MUT molecule, so that an ideal receiver is emulated. Furthermore, the equivalent voltage at the receiver could be also computed to check whether or not the information propagates even in case of fabrication defects. Finally, a *Safe Operating Area (SOA)* could be defined in order to evaluate the fault tolerance of a molecular QCA wire: in the SOA, it is possible to highlight the working points of the receiver that represent all the receiver positions in which a driver displacement is tolerated and

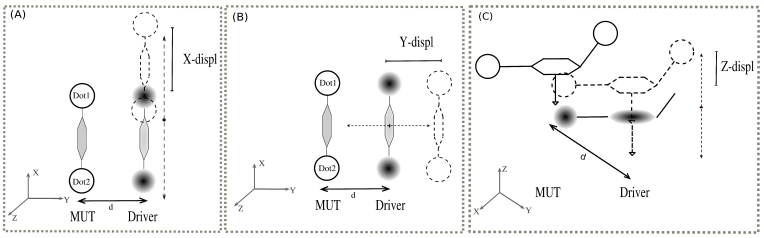


**Fig. 21.** Models of three possible defects in a QCA wire.

the communication through the wire is not compromised. These working points could be computed measuring the equivalent voltage at the receiver and checking whether the receiver could still switch its logic state following the changing logic state of the MUT. In particular, a different SOA could be drawn for each driver displacement on a given area of interest centered on the MUT. The electric field generated by the MUT in the two cases of driver logic state is used to compute the equivalent voltage at the receiver, defined as $V_{rx1}$ and $V_{rx0}$, for the driver logic 1 and 0 respectively. Defining a set of threshold voltages ($V_{th}$) ranging from 0.1 to 1.0 V, a generic point $(x, y)$ of the area could be considered *safe* for any threshold voltage ($V_{th}$) that satisfies simultaneously the two following conditions:

$$V_{rx1}(x, y) > |V_{th}| \tag{10}$$

$$V_{rx0}(x, y) < |V_{th}|. \tag{11}$$

## 3 Simulation results and models

### 3.1 Single molecule characterization

The neutral bis-ferrocene molecule in the ground state has the HOMO that is de-localized along the molecule and mainly on the carbazole as shown in Figure 22(A). The application of an electric field along the X axis (switching field) leads to a localization of the HOMO around one of the two ferrocenes, as shown in Figure 22(B) and (C), depending on the sign of the switching field. Following the methodology adopted in literature [4–6], the HOMO localization could represent the logic state of the molecule and for the bis-ferrocene molecule a write-in system based on electric field seems to work properly [15].

As shown in Figure 23, applying the switching field the charge distribution inside the molecule varies and the molecule exhibits a charge localization in favor of one of the two dots, depending on the sign of the switching field. In particular, with a positive switching field Dot2 (green curve) becomes more positively charged than Dot1 (red curve), while the carbazole charge (Dot3, blue curve) does not significantly vary. Changing the sign of the switching field the

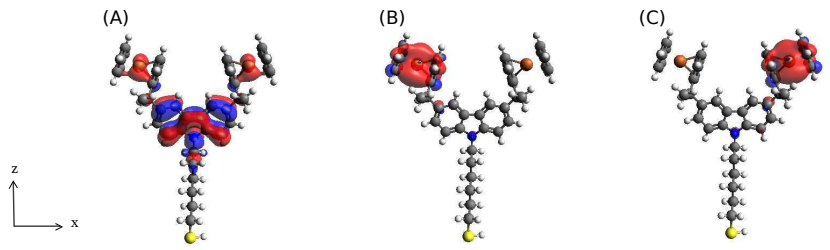


**Fig. 22.** Bis-ferrocene molecule: HOMO localization at (A) the equilibrium and (B, C) in presence of switching field.

situation is dual. For both positive and negative applied field, the displacement of charge between Dot1 and Dot2 is small and this represents a problem in the encoding and identification of the two logic state. Thus, for QCA application it could be necessary to oxidize or reduce the molecule.

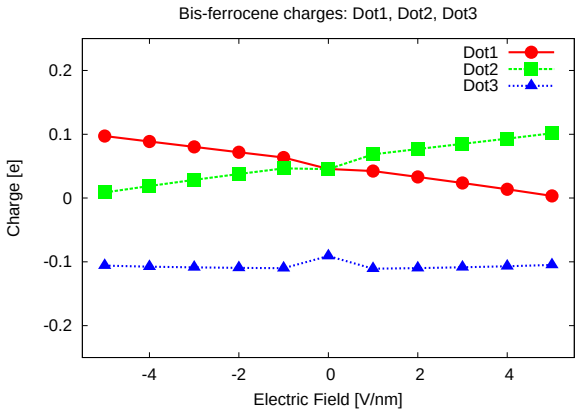


**Fig. 23.** Bis-ferrocene molecule: dot charges as function of the switching field.

Considering the oxidized version of the bis-ferrocene, at the equilibrium the free positive charge is mainly delocalized between the working dots, while the third dot is almost neutral. The application of the switching field moves the positive charge entirely on one of the two dots, depending on the sign of the electric field, and the third central dot remains almost neutral. The trend of the dot charges of the oxidized bis-ferrocene as a function of the switching field are reported in Figure 24: the oxidized bis-ferrocene has a non linear behavior, since for a given value of the switching field the charge distribution "saturates", that means that the whole positive charge is confined in one of the two active dots and even increasing the modulus of the electric field the charge distribution does

not significantly vary. The results shown in Figure 24 are important because they highlight the QCA properties of the bis-ferrocene molecule, as well as the suitability of a write-in system based on electric field.

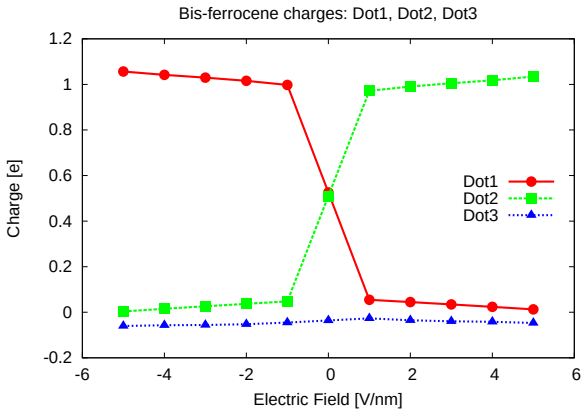


**Fig. 24.** Oxidized bis-ferrocene molecule: dot charges as function of the switching field.

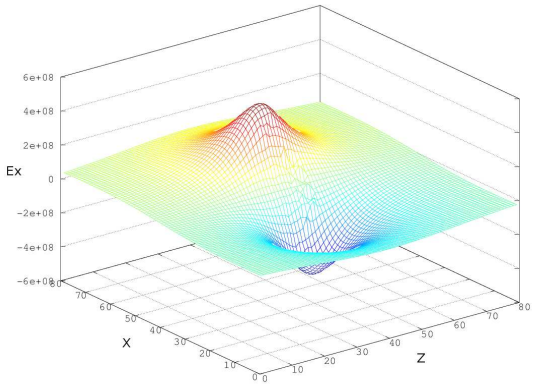


**Fig. 25.** Component X of the electric field generated by the bis-ferrocene at the equilibrium and measured at a distance of 1.0 nm from the molecule.

Given the charge distributions of the oxidized bis-ferrocene in different bias conditions, the generated electric field was computed as second part of the second stage of the analysis flow (post-processing stage described in Section 2.2). In

particular, the component X (parallel to the dot axis) of the electric field ($E_x$) generated by the molecule at the equilibrium was computed considering an ideal receiver placed at the distance of 1.0 nm from the molecule along the Y axis, so that a squared QCA cell could be formed. The values of the electric field modulus are reported in Figure 25 for all the points of the XZ plain.

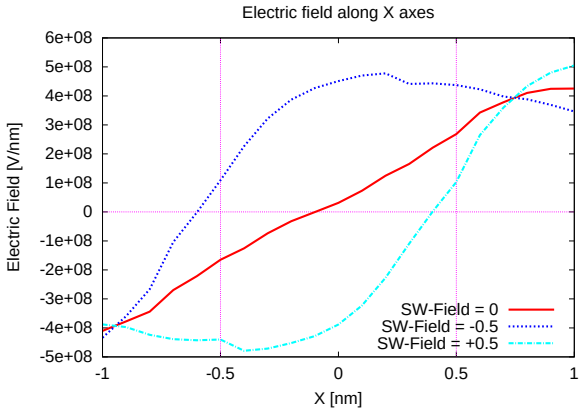


**Fig. 26.** Component X of the electric field generated by the bis-ferrocene in different bias conditions and measured at position of an ideal receiver.

In the same way, the electric field generated by the molecule under the effect of a switching field was computed, and in order to evaluate the actual effect on an ideal receiver, it is necessary to cut the curves along the axis where the active dots of the receiver stand, that means fixing the position of the receiver on the Z axis since the active dots of both the molecule and the receiver lie along the X direction. Figure 26 shows the results for the molecule at the equilibrium (SW-Field = 0, red line) and in two cases of switching field (SW-Field = -0.5 nm and SW-Field = +0.5 nm, respectively green and red line). The two vertical violet lines indicate the width of the receiver, that is equal to 1.0 nm (the width of a bis-ferrocene molecule). In order to evaluate the effects of the electric field on the receiver, the curves has to be considered only along the receiver width. At the equilibrium (red curve) the two dots of the receiver (placed at the edge of the receiver and so where the violet lines stand) are subject to an electric field, whose intensity is almost the same, as well as the direction, but the sign is opposite and so the result is almost null. This means that the molecule at the equilibrium does not influence an ideal receiver. For negative applied switching field (green curve) the positive peak of the generated electric field moves backward and it is centered on the receiver. For this reason, the sign of the electric field that influences the receiver (positive) is opposite with respect to the sign of the switching field applied to the molecule (negative), thus the receiver should encode a logic state opposite to the molecule state. On the contrary, in case of positive switching

field (blue curve) the situation is dual, since the negative peak of the generated electric field is centered on the receiver.

### 3.2 Interaction between two molecules

A complete QCA cell could be implemented aligning two bis-ferrocene molecules with an ideal inter-molecule distance equal to the width of the molecule. For this reason, the further step of this analysis concerns the interaction between molecules: the charge distribution of two nearby molecules was evaluated emulating one of the two molecules with a polarized driver, both in case of neutral and oxidized bis-ferrocene.

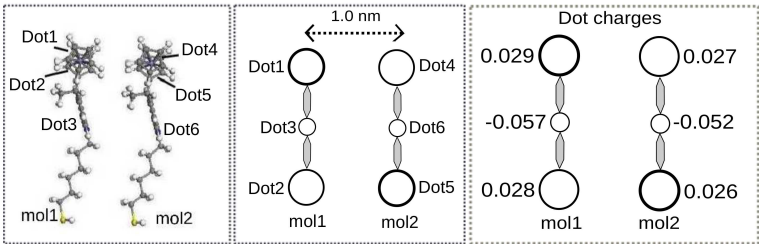


**Fig. 27.** Charge distribution of two nearby bis-ferrocene molecules (complete QCA cell).

In case of two neutral molecules placed at a distance of 1.0 nm, the charge dots at the equilibrium are all almost zero as reported in Figure 27. To model the effects of a polarized driver the single bis-ferrocene molecule was simulated in presence of a system of point charges placed at the reference distance from the molecule. Figure 28 reports the results obtained: considering a neutral bis-ferrocene molecule (Figure 28(A)), the driver was emulated with a positive and a negative charge to maintain the driver neutrality (Figure 28(B)) and the effect on the target molecule is a slight displacement of charge between the working dots (Figure 28(C)). Swapping the two point charges (that means switching the driver logic state) the situation is dual. This means that the molecule interacts with the driver, but the intrinsic properties of the neutral molecule already discussed in the previous section affect also the driver-molecule interaction.

### 3.3 Effect of clock on molecule switching

The next step of the analysis was the simulation of a clock signal in order to evaluate the possibility to enhance or hinder the communication between nearby molecules. In the case of bis-ferrocene molecule, the clock signal could be implemented with an electric field applied along the vertical axis of the molecule. The analysis was performed both on the neutral and the oxidized bis-ferrocene and

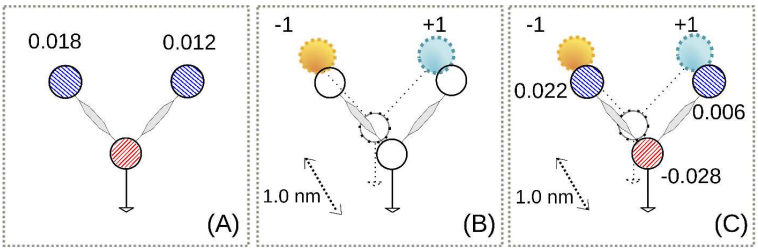


**Fig. 28.** Charge distribution of a bis-ferrocene molecules in presence of a polarized driver.

also in presence of a polarized driver. The molecule was simulated with all its elements and so including the thiol, whose charge is considered as component of the third dot charge.

In case of neutral molecule, the application of a negative clock field generates a displacement of charges inside the molecule and in particular the working dots became negatively charged, while the carbazole charge becomes positive. The charge distribution of the clocked molecule is depicted in Figure 29(B). On the other hand, the application of a positive clock signal leads to a dual configuration in which the working dots have a positive charge, almost equal, and the carbazole becomes negatively charged (Figure 29(C)). In this case, the charge distribution is similar to the charge distribution of an oxidized molecule at the equilibrium, since the working dots have a similar amount of charge, while the carbazole of the clocked neutral molecule compensates the neutrality of the cell.

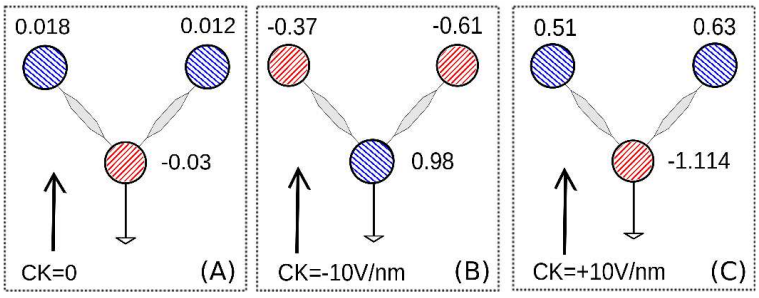


**Fig. 29.** Charge distribution of a clocked bis-ferrocene molecule.

To completely characterize the effects of the clock, a polarized driver was introduced during the simulations, in both the logic state 1 and 0. The results are reported in Figure 30 and show that the clocked molecule reacts better than the non clocked one, since in the former case the displacement of charge between the working dots is more pronounced then in the latter. For this reason, the clock

signal could be used to enhance the charge localization inside a neutral molecule and, so, to help the interaction between neighboring cells.

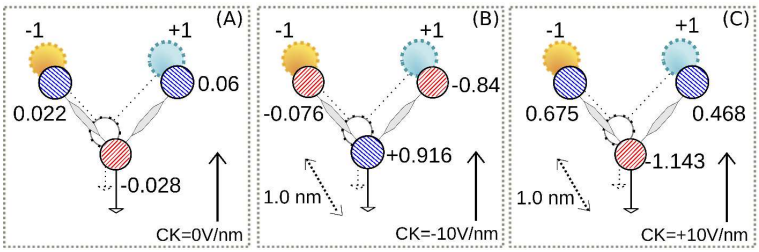


**Fig. 30.** Charge distribution of a clocked bis-ferrocene molecule in presence of a polarized driver.

Finally, thanks to this analysis it was possible to evaluate the properties of the bis-ferrocene molecule as QCA device. As shown by the results discussed here, the molecule is a suitable candidate for QCA technology, especially in its oxidized form. In fact, the oxidized bis-ferrocene exhibits a good charge confinement when a write-in signal is applied and it reacts properly to a polarized driver. Regarding the neutral bis-ferrocene, its performance are lower than the oxidized version, but the application of a clock signal could enhance the charge confinement inside the molecule and then the interaction with a nearby molecule or a polarized driver.

### 3.4 Interaction among molecules in a wire

Following the methodology described in Section 2.2 and concerning the post-processing stage of the analysis flow, the interaction among molecules in a QCA wire was evaluated, considering two inter-molecule distances: the ideal one (1.0 nm) equal to the width of the bis-ferrocene, so that a squared QCA cell is formed, and a lower distance equal to 0.8 nm. In Fig. 31 the charges of the two main dots (Dot1 and Dot2) are reported in case of standard inter-molecule distance: for sake of brevity, only the first part of the wire was reported, considering only five molecules. In this case, the logic state of the molecules alternates along the wire, but the charge displacement between the two dots is smaller and smaller while increasing the number of molecules. In particular the fifth molecule is in an undefined state since the dot charges are almost the same. For this reasons, the logic signal could be considered valid only for the first three molecules, while from the fourth molecule on the state is not defined.

On the other hand, when the molecules are placed at 0.8 nm far from each other, the logic state of the molecules along the wire alternates as well, as shown in Figure 31. Moreover, the difference of charge between the two dots is still huge enough to consider all the molecules in a defined logic state.

As additional figure of merit for this analysis, the electric field generated by the molecules along the wire was computed in both the cases of distance. In

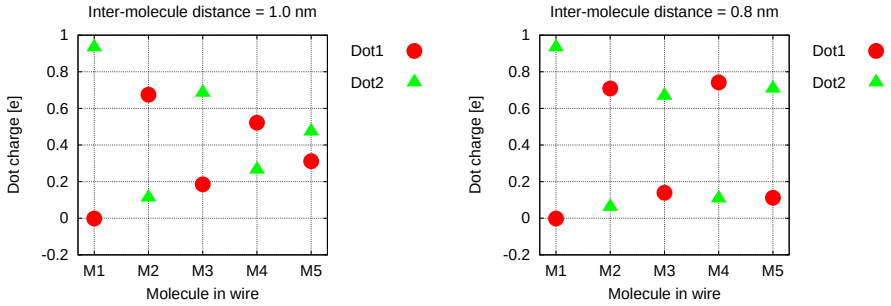


**Fig. 31.** Molecular QCA wire: dot charges of the molecules along the wire with a molecule-molecule distance equal to 1.0 nm.

particular, each molecule along the wire, depending on its logic state, generates an electric field whose absolute value is maximum near the occupied dot. Figure 32 shows a top view of the electric field generated by the first five molecules of the wire, computed at the position of an ideal receiver. The picture shows how the pick of the electric field moves following the position of the free charge inside the molecule, but the intensity of the electric field decreases with increasing number of molecules.

On the contrary, in case of distance equal to 0.8 nm, the positive and negative peaks of the electric fields alternate as well (Figure 33), but the values of the electric field are kept constant for all the molecules, as consequence of the charge distribution inside the molecules.

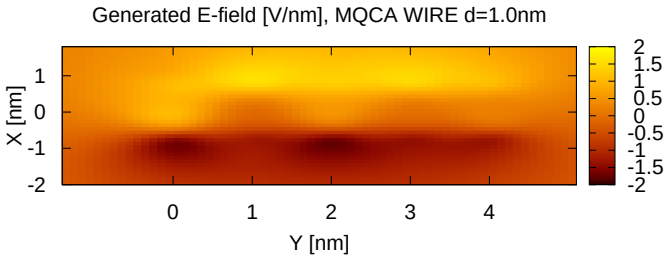


**Fig. 32.** Molecular QCA wire: electric field generated by the molecules along the wire with a molecule-molecule distance equal to 1.0 nm.

These results reveal the strength of the logic interaction in two molecular QCA wires. In particular, the one with the ideal distance for the bis-ferrocene molecule (*d=1.0 nm*) shows a degradation already at the fourth molecule, while in case of *d=0.8 nm* the signal seems to be preserved for a great number of

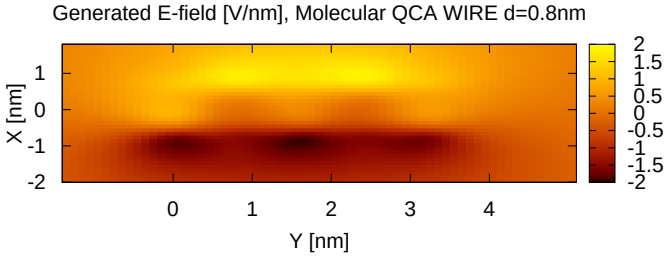


**Fig. 33.** Molecular QCA wire: electric field generated by the molecules along the wire with a molecule-molecule distance equal to 0.8 nm.

molecules. This means that the molecular QCA wire could be built with an inter-molecule distance lower than the ideal one, in order to ensure the information propagation through the wire.

### 3.5 Fault tolerance analysis based on real fabrication defects

Considering the technological steps of the fabrication of a molecular QCA wire made of bis-ferrocenes [16, 18] and the classification of the possible defects that may occur reported in Section 2, a fault tolerance analysis of the bis-ferrocene wire was carried out. As described in Section 2, the evaluation was performed computing the charge distribution inside a bis-ferrocene molecule (MUT) in presence of a driver, for different positions of the driver (ideal and subject to a defect).

Figure 34 displays the results for the driver shifting along the vertical axes, defined as Z-displ. The graph includes the results for three different distances from the MUT (equivalent to three values of Y-displ), considering the driver in both the logic state. The charge difference between the two dots of the MUT decreases when the value of Z-displ is incremented, which is enhanced for longer distances from the molecule (higher Y-displ). In particular, in the range related to the roughness of the gold substrate inside a grain ($\pm 0.2 \div 0.4nm$) the molecule still works properly, that means that the free positive charge is mainly localized on one of the two dots, encoding a valid logic state. On the contrary, when the driver-MUT interaction is at the interface between two gold grains (equivalent to $Z - displ = \pm 2.0nm$) the molecule is in an undefined state, because the charge of the two dots is almost the same.

For what concerns the driver misalignment with the respect to the two dots of the MUT (X-displ), the dot charges are reported in Fig. 35 for the ideal distance between the MUT and the driver (Y-displ = 0). In this case, both the driver logic state at 1 and at 0 reported simultaneously, in order to check immediately the MUT capability to encode the binary information for a specific driver position. In particular, for a given X-displ value it is possible to check if the positive charge inside the MUT moves between the two dots when the driver changes its

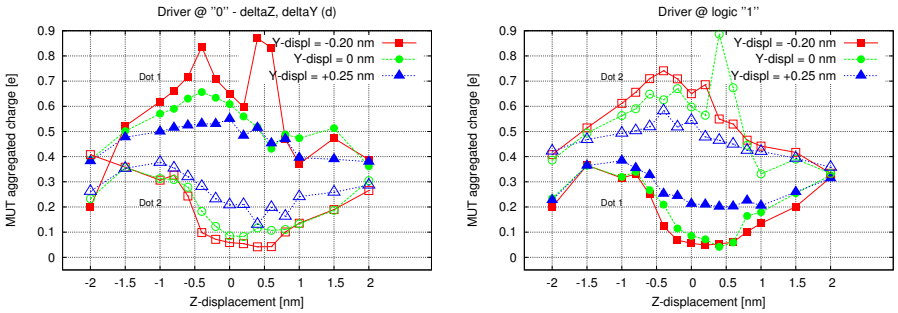


**Fig. 34.** MUT dot charges as function of the driver vertical shifting (Z-displ), in three case of driver-molecule distance (Y-displ).

state from 1 to 0 and the difference between them is great enough to consider the MUT in a valid logic state. Figure 35 reveals that in some cases of driver misalignment the interaction with the MUT is still preserved.

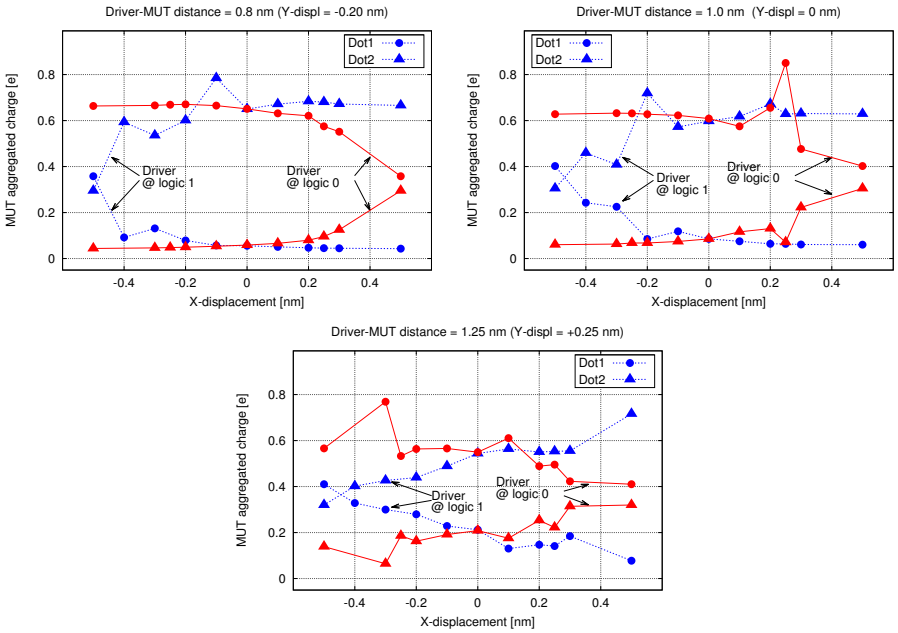


**Fig. 35.** MUT dot charges as function of the driver misalignments (X-displ), in three case of driver-molecule distance (Y-displ).

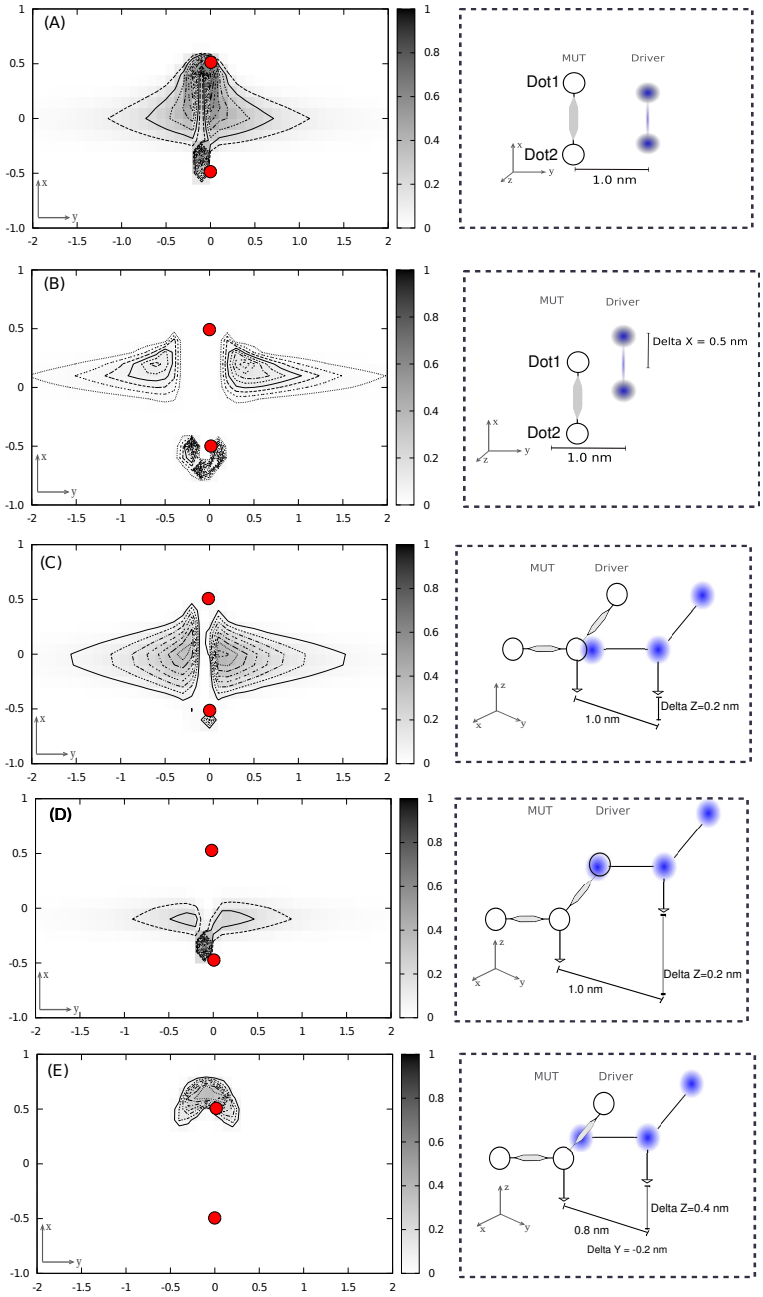


**Fig. 36.** Charge distribution of a clocked bis-ferrocene molecule in presence of a polarized driver.

Finally, the simultaneous concurrency of driver and receiver defects were analyzed in order to draw a Safe Operating Area (SOA), that shows all the positions of the receiver that do not prevent the communication among the molecules. The results are reported in Figure 36, where different corner cases of driver defects are considered: ideal position (no defects), lateral misalignment and vertical shift at the ideal driver-molecule distance, vertical shift at a lower driver-molecule distance. The results in case of ideal position of the driver are shown in Figure 36(A): the positions (the barycenter of the molecule) of the receiver, in which it could still encode the two logic states, are highlighted. Two red circles indicate the working dot of the MUT, that was kept fixed. In case of driver misalignment equal to *X-displ = 0.5 nm*, the region where the receiver could be safely placed (Figure 36(B)) is a little bit wider than the previous case, especially in the Y direction, but the equivalent voltage at the receiver is quite lower. A vertical shifting of the driver due to the roughness of the substrate (*Z-displ = 0.2 nm*) is reflected at the receiver level with a SOA that includes a wide range of both misalignments and higher distances from the molecule (Figure 36(C)). In this case, the values of the equivalent voltage at the receiver are intermediate, confirming again that the gold roughness (0.20 nm $\pm$ 0.1 nm) obtained at the experimental level does not affect the information propagation. In case of a bigger vertical shifting of the driver (*Z-displ = 0.8 nm*), the charge distribution of the molecule is such that the SOA for the receiver is quite limited, as shown in Figure 36(D). Finally, the simultaneous concurrency of a vertical shift and a variation in the driver-molecule distance (*Z-displ = 0.4 nm* and *Y-displ = -0.2 nm*) is quantified at the receiver level in a very small SOA, depicted in Figure 36(E), mainly localized near the molecule, with low values of equivalent voltage.

In summary, this analysis reveals that the tolerance of the QCA wire to some possible defects in the fabrication of the QCA wire is quite good. In addition, the results obtained and the data highlighted in Figure 36 give an important feedback to the technologist about which are the critical points and which could be the improvement to assure a correct information propagation.

## 4 Conclusions

We summarized the most important characteristics of molecules currently under study as potential candidate as QCA devices. In particular we focused and discussed our method aimed at solving one of the gap that is preventing those molecules from being exhaustively studied from an electronic point of view and used as elements in a circuit. We indeed present our two stages methodology, which starts form ab-initio simulations in several conditions followed by a second stage where post-processing is executed and electrostatic inspections are performed. The outcome is twofold. First, we improve the understanding of a MQCA wire based on a bisferrocene molecule and assess the conditions under which it can be used as well as the constraints the technological process should be subjected to. Second, we propose a method to systematically and thoroughly

study this and other molecules to be used as perspective MQCA devices. Though several steps are still necessary, our contribution enables the study of MQCA with an electronic perspective, allowing then to move from the single device level to a circuit level, still maintaining a strong link with the technological aspects.

## References


1. C.S. Lent, P.D. Tougaw, W. Porod and G.H. Bernstein, *Quantum cellular automata*, Nanotechnology, vol. 4, pp. 49-57, 1993.
2. V. Vankamamidi, M. Ottavi, F. Lombardi, *Clocking and Cell Placement for QCA*, IEEE-NANO 2006, vol. 1, pp. 343- 346, 2006.
3. M. Graziano, M. Vacca, A. Chiolerio, M. Zamboni, "A NCL-HDL Snake-Clock Based Magnetic QCA Architecture", IEEE Transaction on Nanotechnology, vol. 10 n. 5, pp. 1141-1149.
4. K. Hennessy and C.S. Lent, *Clocking of molecular quantum-dot cellular automata*, Journal of Vacuum Science and Technology B, vol. 19, pp. 1752-1755, 2001.
5. C.S. Lent and B. Isaksen, *Clocked molecular quantum-dot cellular automata*, Electron Devices, IEEE Transactions on, vol. 50, pp. 1890-1896, 2003.
6. C.S. Lent, B. Isaksen and M. Lieberman, *Molecular quantum-dot cellular automata*, J. Am. Chem. Soc., vol. 125, pp. 1056-1063, 2003.
7. H. Qi, S. Sharma, Z. Li, G.L. Snider, A.O. Orlov, C.S. Lent and T.P. Fehlner, *Molecular quantum cellular automata cells. Electric field driven switching of a silicon surface bound array of vertically oriented two-dot molecular quantum cellular automata*, J. Am. Chem. Soc., vol. 125, pp. 15250-15259, 2003.
8. J. Jiao, G.J. Long, L. Rebbouh, F. Grandjean, A.M. Beatty and T.P. Fehlner, *Properties of a mixed-valence (Fe-II)(2)(Fe-III)(2) square cell for utilization in the quantum cellular automata paradigm for molecular electronics*, J. Am. Chem. Soc., vol. 127, pp. 17819-17831, 2005.
9. Y. Lu and C.S. Lent, *Theoretical Study of Molecular Quantum-Dot Cellular Automata*, Journal of Computational Electronics, vol. 4, pp. 115-118, 2005.
10. Y. Lu, M. Liu and C.S. Lent, *Molecular quantum-dot cellular automata: From molecular structure to circuit dynamics*, Journal of Applied Physics, vol. 102, 2007.
11. Y. Lu and C.S. Lent, *Self-doping of molecular quantum-dot cellular automata: mixed valence zwitterions*, Phys. Chem. Chem. Phys., vol. 13, pp. 14928-14936, 2011.
12. X. Wang and J. Ma, *Electron switch in the double-cage fluorinated fullerene anions: new candidates for molecular quantum-dot cellular automata*, Phys. Chem. Chem. Phys., 2011, vol. 13, pp. 16134-16137, 2011
13. L. Zoli, *Active bis-ferrocene molecules as unit for molecular computation*, PhD dissertation, 2010.
14. V. Arima, M. Iurlo, L. Zoli, S. Kumar, M. Piacenza, F. Della Sala, F. Matino, G. Maruccio, R. Rinaldi, F. Paolucci, M. Marcaccio, P.G. Cozzi and A.P. Bramanti, *Toward quantum-dot cellular automata units: thiolated-carbazole linked bisferrocenes*, Nanoscale, vol. 4, pp. 813-823, 2012
15. A. Pulimeno, M. Graziano, C. Abrardi, D. Demarchi, and G. Piccinini, *Molecular QCA: A write-in system based on electric fields*, IEEE Nanoelectronics Conference (INEC), June 2011.
16. A. Pulimeno, M. Graziano, D. Demarchi, and G. Piccinini, *Towards a molecular QCA wire: simulation of write-in and read-out systems*, Solid State Electronics, Elsevier, vol. 77, pp. 101-107, 2012.

17. A. Pulimeno, M. Graziano, and G. Piccinini, *Molecule Interaction for QCA Computation*, IEEE NANO2012 12th International Conference on Nanotechnology, Birmingham (UK), 20-23 August 2012.
18. A. Pulimeno, M. Graziano, A. Sanginario, V. Cauda, D. Demarchi, and G. Piccinini, *Bis-ferrocene molecular QCA wire: ab-initio simulations of fabrication driven fault tolerance*, IEEE Transactions on Nanotechnology, in press.
19. X. Wang, S. Chen, J. Wen and J. Ma, *Exploring the Possibility of Noncovalently Surface Bound Molecular Quantum-Dot Cellular Automata: Theoretical Simulations of Deposition of Double-Cage Fluorinated Fullerenes on Ag(100) Surface*, J. Phys. Chem. C, 2012.
20. Y. Lu, R. Quardokus, C.S. Lent, F. Justaud, C. Lapinte and A. Kandel, *Charge localization in isolated mixed-valence complexes: An STM and theoretical study*, J. Am. Chem. Soc., vol. 132, pp. 13519-13524, 2010.
21. R. Quardokus, Y. Lu, N.A. Wasio, C.S. Lent, F. Justaud, C. Lapinte and S.A. Kandel, *Through-Bond versus Through-Space Coupling in Mixed-Valence Molecules: Observation of Electron Localization at the Single-Molecule Scale*, J. Am. Chem. Soc., vol. 134, pp. 1710-1714, 2012.
22. F. Mohn, L. Gross, N. Moll and G. Meyer, *Imaging the charge distribution within a single molecule*, Nature Nanotechnology, vol. 7, pp. 227-231, 2012.
23. U. C. Singh, P. A. Kollman, *An approach to computing electrostatic charges for molecules*, Journal on Computational Chemistry, vol. 5, pp 129 - 145, 1984.